Journal of Carbon Research

MDPI

Article

A New Monohydrogen Phosphate-Selective Carbon Composite Membrane Electrode for Soil Water Samples

Ozlem Tavukcuoglu [1,*], Vildan Erci [2], Fatih Ciftci [3,4,*], Ibrahim Isildak [5] and Muhammed Zahid Kasapoglu [6]

[1] Department of Biochemistry, Faculty of Hamidiye Pharmacy, University of Health Sciences, Istanbul 34668, Turkey
[2] Department of Soil Science and Nutrition, Faculty of Agriculture, Selcuk University, Konya 42130, Turkey; vildanerci@selcuk.edu.tr
[3] Department of Biomedical Engineering, Fatih Sultan Mehmet Vakıf University, Istanbul 34015, Turkey
[4] Department of Technology Transfer Office, Fatih Sultan Mehmet Vakıf University, Istanbul 34015, Turkey
[5] Department of Bioengineering, Faculty of Chemical and Metallurgical Engineering, Yildiz Technical University, Istanbul 34220, Turkey; isildak@yildiz.edu.tr
[6] Institute of Nanotechnology and Biotechnology, İstanbul University-Cerrahpaşa, Istanbul 34320, Turkey; muhammed.kasapoglu@iuc.edu.tr
* Correspondence: ozlemoztolan@gmail.com (O.T.); faciftcii@gmail.com or fciftci@fsm.edu.tr (F.C.)

Abstract: This study focused on developing a novel composite phosphate-selective electrode for on-site and real-time applications using a silver polyglutaraldehyde phosphate and carbon nanotube (CNT) matrix. CNT-silver polyglutaraldehyde phosphate compound was synthesized and characterized using Fourier-transform infrared spectroscopy (FTIR), scanning electron microscopy (SEM), X-ray diffraction (XRD), and thermogravimetric analysis (TGA). The potentiometric performance of the composite phosphate-selective electrode was then investigated. The results demonstrated that the composite phosphate-selective electrode exhibited good sensitivity, with a linear response in the concentration range of 1.0×10^{-4} to 1.0×10^{-2} M for phosphate ions. The electrode also showed high selectivity towards phosphate ions compared to other anions, such as chloride and nitrate. Additionally, the electrode displayed a quick response time of less than 15 s, making it suitable for real-time measurements. The electrode was applied to surface and soil water samples. The results obtained from the water samples showed a strong correlation with those obtained from the preferred spectrophotometry method, highlighting the potential of the developed electrode for on-site and continuous monitoring of phosphate and offering an efficient and practical solution for various fields that require phosphate detection.

Keywords: composite matrix; phosphate-selective electrode; solid contact; soil analysis

Academic Editor: Athanasia Tolkou

Received: 5 December 2024
Revised: 22 February 2025
Accepted: 26 February 2025
Published: 1 March 2025

Citation: Tavukcuoglu, O.; Erci, V.; Ciftci, F.; Isildak, I.; Kasapoglu, M.Z. A New Monohydrogen Phosphate-Selective Carbon Composite Membrane Electrode for Soil Water Samples. *C* **2025**, *11*, 18. https://doi.org/10.3390/c11010018

1. Introduction

The development of phosphate-selective electrodes has gained significant attention due to the increasing need for the efficient, reliable, and cost-effective detection of phosphate ions across various applications, including in environmental monitoring, agriculture, and biomedical analysis [1–3]. Phosphates are essential for all living organisms, existing in both inorganic and organic forms, with orthophosphates (HPO_4^{2-} and $H_2PO_4^-$) being the most prevalent in natural environments [4]. They play critical roles in biological functions such as energy metabolism, genetic information storage, and cell signaling [4–6].

While phosphates are vital for human health and agricultural productivity, their overuse, particularly through phosphate-based fertilizers, poses serious environmental challenges. Phosphate pollution significantly degrades groundwater and surface water

quality, leading to eutrophication, characterized by excessive algal blooms that disrupt aquatic ecosystems. The leaching of phosphates into water bodies due to improper fertilizer application necessitates substantial investments in wastewater treatment systems to mitigate these impacts. Therefore, monitoring phosphate levels in natural water sources and agricultural soils is crucial for maintaining water quality and optimizing agricultural outputs, which can help prevent economic losses for farmers [4,7,8].

Electrochemical sensors have emerged as a promising solution for phosphate monitoring, offering a high sensitivity for detecting trace levels of phosphates and other nutrients in soil and water samples [9–17]. These sensors provide rapid results, enabling real-time monitoring essential for dynamic environmental assessments. Their cost-effectiveness and compact design make them suitable for large-scale agricultural applications, allowing for in-field measurements without the need for extensive laboratory setups. Moreover, electrochemical sensors can be customized for specific ions, achieving high selectivity even in complex soil matrices. This selectivity is crucial for accurate monitoring in environments where multiple ions may be present. Compared to traditional chemical analysis methods, electrochemical techniques typically require minimal sample preparation, reducing analysis time and the risk of contamination. Additionally, these methods are environmentally friendly, as they generally consume fewer reagents and generate less waste, aligning with sustainable practices in environmental monitoring [18].

The growing need for the rapid and on-site analysis of environmental samples has driven the development of ion-selective electrode (ISE) technology for phosphate measurement [19–22]. ISE technology enables fast, selective, and quantitative measurement of phosphate levels [18]. Researchers have utilized various nanomaterials to enhance the sensitivity and stability of ion-selective electrodes for phosphate determination, with carbon nanotubes (CNTs) being widely employed due to their large surface area, high electrical conductivity, and chemical stability [23–27].

This study focuses on developing a composite matrix potentiometric electrode that utilizes carbon nanotube (CNT) and silver polyglutaraldehyde phosphate (Ag-pGAP) for the precise detection of monohydrogen phosphate ions. The synthesis and characterization of this composite material are outlined, alongside an assessment of the potentiometric performance of the phosphate-selective electrode and an exploration of its commercial viability and scalability. A thorough examination of the composite membrane matrix, which includes Ag-pGAP and CNT, will be conducted using various analytical techniques, including Fourier-transform infrared spectroscopy (FTIR), scanning electron microscopy (SEM), X-ray diffraction (XRD), thermogravimetric analysis (TG-DTG), and differential thermal analysis (DTA). Furthermore, the potentiometric performance attributes of the optimized electrode, such as selectivity and sensitivity, will be rigorously evaluated. The practical applicability of the developed phosphate-selective electrode will be illustrated through the measurement of phosphate concentrations in wastewater and soil samples [1]. Consequently, this planned study aims to provide an in-depth understanding of how a novel composite material, comprising Ag-pGAP and CNT, can improve the functionality of phosphate-selective electrodes. The findings will pave the way for the development of practical and scalable sensors for detecting phosphate ions, effectively addressing significant challenges related to sensitivity, selectivity, and stability.

2. Materials and Methods

2.1. Materials and Solutions

Thiourea dioxide, tetrahydrofuran (THF), silver (I) sulfide, Tris buffer solution (pH 7.0), copper (I) sulfide, and Kelowna extractant solution containing 0.25 mol/L CH_3COOH and 0.015 mol/L NH_4F were purchased from Sigma-Aldrich (St. Louis, MO, USA); glu-

taraldehyde and graphite were purchased from Fluka (Buchs, Switzerland); CNT was purchased from www.us-nano.com (Houston, TX, USA); silver nitrate was purchased from Carlo Erba (Milan, Italy); disodium monohydrogen phosphate was purchased from Merck (Darmstadt, Germany); hardener was purchased from Bayer (Leverkusen, Germany); and epoxy was purchased from Araldite (Basel, Switzerland). All chemicals and sodium salts of the anions used were of analytical grade. Throughout the experimental studies, double-distilled deionized water was used. A stock disodium monohydrogen phosphate solution (1.0×10^{-1} M) was prepared. Dilute solutions (1.0×10^{-1}–1.0×10^{-5} M) of disodium monohydrogen phosphate were then prepared by appropriate dilution of the stock solution with deionized water.

2.2. Synthesis of Silver Polyglutaraldehyde Phosphate (Ag-pGAP)

In the synthesis process, 7.4 g of thiourea dioxide and 21 g of 50% glutaraldehyde by weight were mixed in a flask. The mixture was then heated in an oil bath at 50 °C for 2 h, forming a light yellow polyglutaraldehyde dissolved in water. Subsequently, 230 mL of a 0.2 M solution of silver nitrate ($AgNO_3$) was added to the mixture, forming a silver complex. To precipitate Ag-pGAP, a dropwise addition of a 10^{-1} M Na_2HPO_4 solution was performed into the resulting complex solution. The precipitate was then washed with water and dried.

2.3. Characterization

The morphology of the silver polyglutaraldehyde phosphate, CNT, and CNT/Ag-pGAP used in the composite matrix was observed and examined using a Zeiss EVO/LS10 scanning electron microscope (SEM) (Carl Zeiss AG, Oberkochen, Germany). X-ray diffraction (XRD) patterns were recorded at ambient temperatures on an X'Pert XRD Philips Panalytical X'Pert Pro diffractometer (Malvern Panalytical, Almelo, The Netherlands) using Ni-filtered CuKα radiation (λ = 1.54059 Å; 45 kV and 40 mA). Fourier-transform infrared spectroscopy (FTIR) spectra of the samples were collected in the 4000–400 cm^{-1} region using a Shimadzu Corp IrPrestige-21 spectrophotometer (Shimadzu Corporation, Kyoto, Japan) with a resolution of 4 cm^{-1}. Thermal analysis curves (TG/DTG, DTA) were monitored using a TA Instruments SDT Q600 apparatus (TA Instruments, New Castle, DE, USA) in a dynamic air atmosphere with a heating rate of 10 °C min^{-1}, using platinum crucibles with a mass of approximately 10 mg, and a temperature range of 0–800 °C. Calcinated α-alumina was taken as the reference.

2.4. Fabrication of the Electrode

The composite membrane electrodes were prepared using the synthesized Ag-pGAP complex. The membrane compositions used with silver sulfide, copper sulfide, and epoxy are also listed in Table 1. The specific composition of the electrode, as shown in Table 1, was selected to optimize performance characteristics, including stability, sensitivity, and selectivity. The chosen materials and their ratios could reflect a carefully balanced compromise that enhanced the electrode's performance in detecting phosphate ions, while minimizing interference and ensuring long-term functionality. Each membrane mixture was homogeneously stirred with the appropriate amount of THF on a watch glass. Using a high-speed mechanical drill system with inserted bit for mixing, carbon nanotubes (CNTs) were well dispersed throughout the membrane matrix. Subsequently, the mixtures were compressed into plastic pipes and dried at room temperature.

Table 1. Ratios of composite phosphate electrodes prepared with Ag-pGAP.

No.	CNT (mg)	Ag-pGAP (mg)	Silver Sulfide (Ag_2S) (mg)	Copper Sulfide (Cu_2S) (mg)	Epoxy (mg)
1	100	10	80	10	800
2	100	10	80	10	600
3	100	10	80	10	400
4	100	10	80	10	200
5	–	11	55	–	34

Thin sections were extracted from the drying tubes and affixed to the end of a copper wire of appropriate length (15 cm, 0.5 mm thickness) using a solid contact material. This solid contact material was created by thoroughly dissolving a mixture consisting of 50% (w/w) graphite, 35% (w/w) epoxy, and 15% (w/w) hardener in a suitable amount of THF. After allowing it to dry for 5 h, the electrodes were insulated with a strong adhesive similar to "Patex" to prepare them for measurement.

2.5. Potentiometric Measurements

Potentiometric measurements were carried out using a multi-channel potentiometer developed by Medisen Medical Technologies Research and Development Ind. Co., Ltd., in Istanbul, Turkey. An Elit solid-state Ag/AgCl dual-junction reference electrode with a lithium acetate internal reference solution was employed for these measurements.

2.6. Statistical Analysis

In this study, the Bland–Altman method and regression analysis were utilized for 30 soil samples to plot the differences against the averages of the measurements obtained from the two distinct methods, allowing for the examination of any relationship between the differences and the averages to compare the outcomes for the same samples. If the differences exhibited a normal distribution, they were expected to be randomly distributed around zero, with 95% falling between the limits of agreement. The Bland–Altman method was implemented using the Origin package program, while the regression analysis was conducted using the MINITAB package program. Additionally, this study utilized the concept of "agreement boundaries" within the Bland–Altman method. If the differences followed a normal distribution, the differences were expected to be randomly distributed around zero, with 95% falling between "$\bar{d} - 1.96$ s and $\bar{d} + 1.96$ s". In this method, the range "$\bar{d} \pm 1.96$ s" refers to "limits of agreement". Furthermore, this study considered the use of regression analysis for calibrating one measurement against another or detecting bias between two measurement methods.

The practical applicability of the composite phosphate-selective electrode was further assessed for analyzing soil surface water samples obtained from three different agricultural areas near Istanbul. To validate the correlation between the two methods, statistical tests such as Student's *t*-test and Fisher's F-test were employed, with calculated values provided.

3. Results and Discussion

3.1. FTIR Analysis

Figure 1a shows the FTIR spectrum for Ag-pGAP, CNT, and the CNT/Ag-pGAP composite. In the FTIR spectrum of silver polyglutaraldehyde phosphate (Ag-pGAP), we observed a significant absorption band between 1740 and 1725 cm^{-1}, associated with C=O stretching [28]. Additionally, the peaks at 2850 and 2750 cm^{-1} indicate C-H stretching related to the aldehyde (-CHO) group. A peak at 2920 cm^{-1} suggests the presence of

silver metal centers. Notably, the intensity of the hydroxyl (OH^-) species was prominently observed around 3450 and 3655 cm^{-1} [29]. When examining the FTIR spectra of CNT and CNT/Ag-pGAP, only minor differences were noted. This is likely due to the low weight percentage (<10%) of Ag-pGAP in the composite. The spectrum is primarily dominated by intense and broad absorption bands from the CNT, which may have obscured the weaker signals from the functional groups of Ag-pGAP. However, the weak split peaks observed at 900 and 950 cm^{-1} in the CNT/Ag-pGAP spectrum indicate the presence of P-O and P-C bonds. This suggests successful bonding between the carbon and phosphorus atoms in CNT and Ag-pGAP. Although these peaks are subtle, they are characteristic of phosphoryl and phosphonate groups, confirming the presence of Ag-pGAP even at low concentrations.

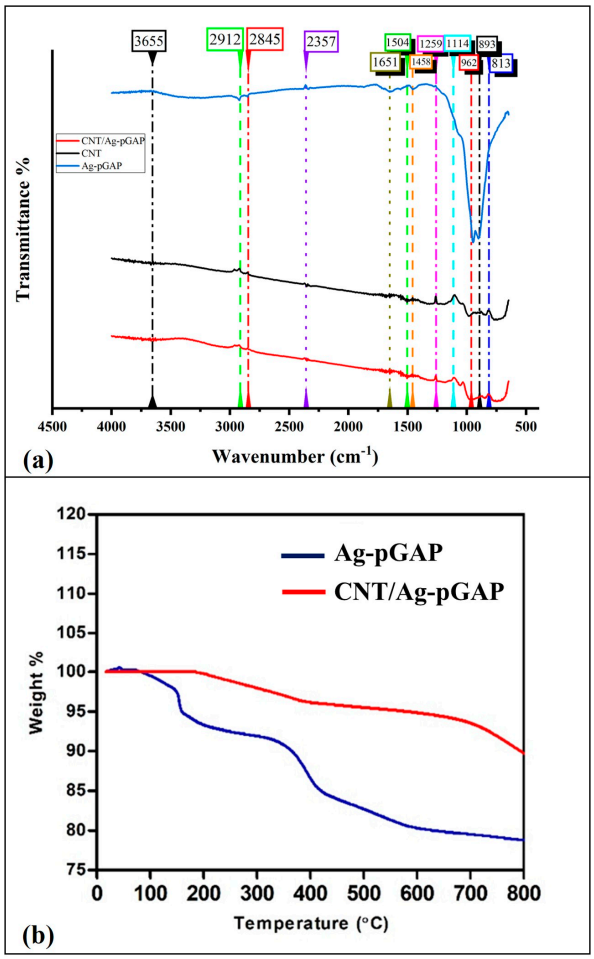

Figure 1. (**a**) FTIR spectrum of Ag-pGAP, CNT, and CNT-Ag-pGAP. (**b**) TGA graphs of Ag-pGAP and CNT-Ag-pGAP.

3.2. Thermogravimetric Analysis

The thermogravimetric behavior of Ag-pGAP and CNT/Ag-pGAP was investigated. The thermogravimetric curves depicting their behavior are shown in Figure 1b. The graphs show that Ag-pGAP experienced weight loss after 120 °C, while CNT/Ag-pGAP compound exhibited weight loss after 200 °C. Complex structures containing metals are known to be stable up to 150 °C, but tend to break down into smaller fragments beyond this temperature. This indicates that CNT/Ag-pGAP behaves like a stable complex. Weight losses between 150 and 600 °C are believed to arise from the degradation of the polyglutaraldehyde phosphate structure. In contrast, CNT/Ag-pGAP shows limited weight loss in this temperature range, suggesting the mixture's high stability. At the final temperature (800 °C), the residues are predicted to have originated from the "silver" content in the

Ag-pGAP structure (77%) and both the "silver and CNT" content in the CNT/Ag-pGAP structure (88%).

3.3. SEM Analysis

Figure 2 presents SEM images of the silver polyglutaraldehyde phosphate (Ag-pGAP), carbon nanotube (CNT), and CNT/Ag-pGAP compounds at various magnifications. The micrographs indicate that Ag-pGAP has an amorphous structure, with silver appearing as tiny particles (Figure 2a). In Figure 2b, the CNT structures are clearly visible with smooth surfaces, showcasing their pristine morphology. In contrast, the SEM image of the CNT/Ag-pGAP composite (Figure 2c) retains the CNT structures but shows a clouded and less defined surface compared to Figure 2b.

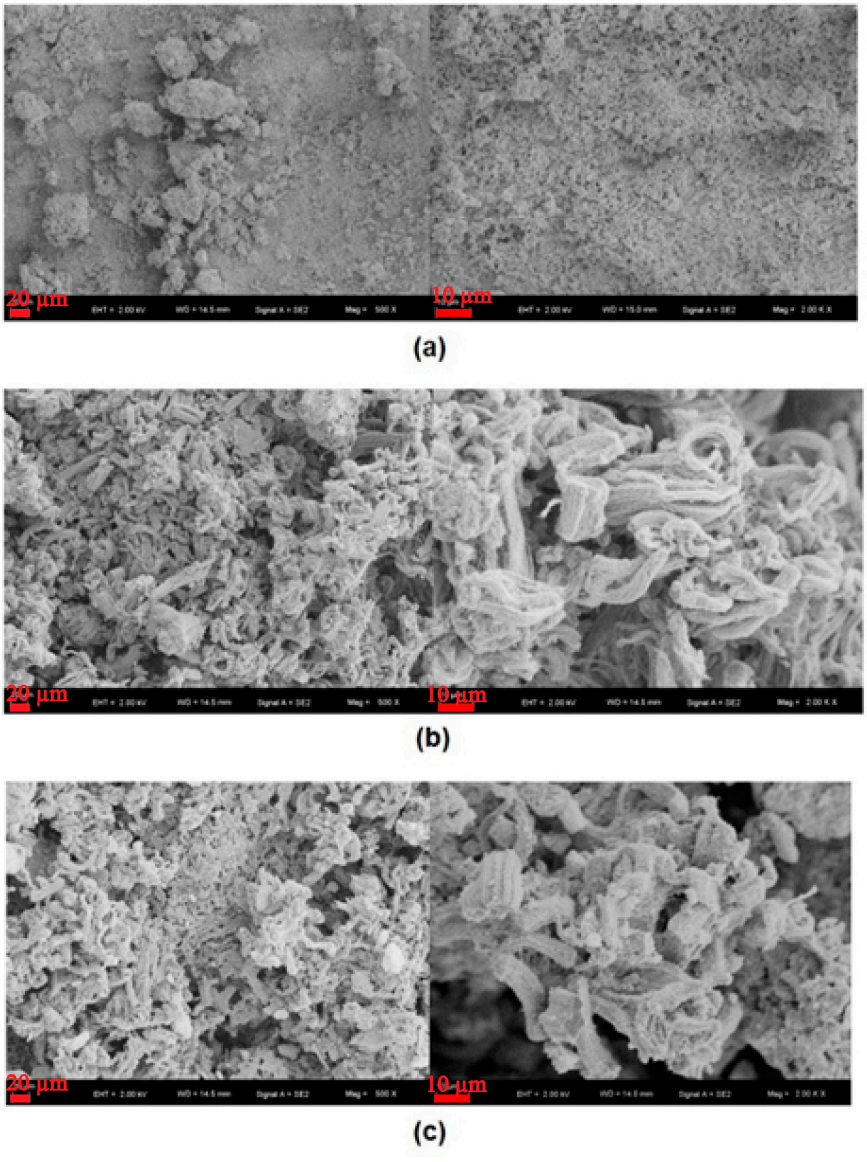

Figure 2. SEM images of (**a**) Ag-pGAP, (**b**) CNT, and (**c**) CNT/Ag-pGAP.

This clouded appearance results from a thin, uniform layer of Ag-pGAP coating the CNTs, which slightly blurs the contours of the nanotubes. Since the Ag-pGAP layer is extremely thin—likely at the nanoscale—its overall morphology remains largely unchanged, but its surface texture experiences subtle alterations. The differences between Figure 2b,c can be challenging to discern due to the thin and homogeneous nature of the Ag-pGAP coating, which does not significantly impact its tubular structure but does affect surface

roughness and texture. Additionally, the clouded surface and slight increase in agglomeration seen in Figure 2c suggest enhanced interactions between the tubes, implying that Ag-pGAP acts as a binding agent.

Given the nanoscale thickness of the Ag-pGAP layer, SEM imaging may have caused a struggle to distinguish the coating from the CNT substrate. This limitation arose from the resolution constraints of SEM in detecting ultrathin, amorphous layers. Nevertheless, the observed clouded surface and slight textural changes provide indirect evidence of the coating, aligning with findings from previous studies, which showed similar challenges in visualizing thin polymeric coatings using SEM [30,31].

3.4. XRD Analysis

The X-ray diffraction spectra of silver polyglutaraldehyde phosphate, CNT, and CNT/Ag-pGAP are shown in Figure 3. The obtained spectra exhibit strong intensity diffraction peaks. In the spectra of the CNT and CNT/Ag-pGAP samples, the peaks observed at approximately 26, 45, 52, and 73 can be attributed to CNT reflections. The broad peaks observed in the spectra indicate that the carbon nanotubes had small dimensions. In the spectrum of CNT/Ag-pGAP, the peaks observed at 31, 33, and 380, along with significant reductions in peak intensities compared to the CNT spectrum, indicate that Ag-pGAP was homogeneously adhered to and surrounded by the CNT surface.

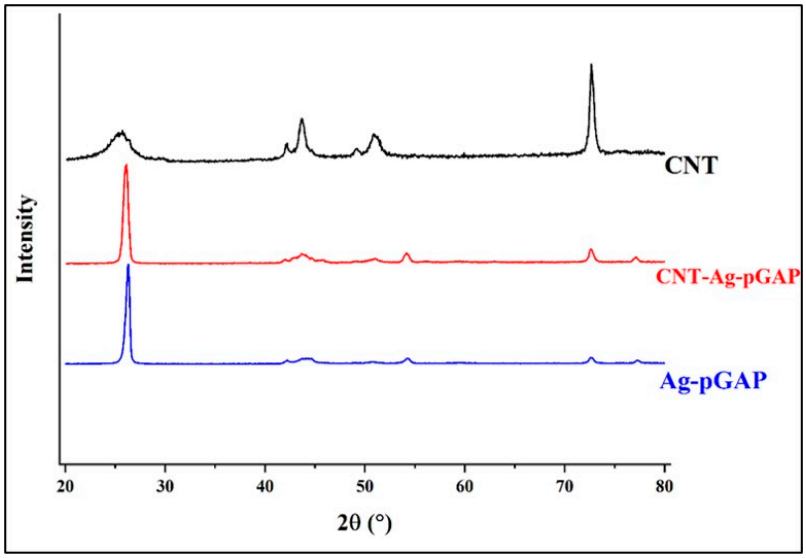

Figure 3. XRD spectra of Ag-pGAP, CNT, and CNT/Ag-pGAP.

3.5. Potentiometric Performance of the Electrode

The electrode membranes, containing Ag-pGAP as an ionophore, demonstrated sensitive responses to HPO_4^{2-} concentrations ranging from 10^{-5} to 10^{-1} mol/L in Tris buffer at pH 8.0. Interestingly, the electrodes exhibited minimal sensitivity to phosphate when Kelowna soil extractant was used as the base solution. In the Kelowna solution, the electrode displayed a sensitive response to HPO_4^{2-} concentrations spanning from 10^{-5} to 10^{-1} mol/L for total phosphate concentration, with a detection limit of 10^{-5} mol/L. This detection range encompasses the typical soil phosphorus concentration range in soil water samples. The electrode's selectivity was deemed satisfactory for measuring phosphates in the presence of six interfering ions, including Cl^-, CH_3COO^-, Cu^{2+}, SO_4^{2-}, HCO_3^-, and NO_3^-, with the electrodes exhibiting significantly higher responsiveness to phosphate compared to the interfering ions. To mitigate any pH influence, the pH levels of the tested solutions were standardized across various tested phosphate concentrations, maintaining the Kelowna solution at pH 8.0, with pH adjustments monitored using an Orion pH meter.

The Kelowna extraction for available and total dissolved P was conducted following the protocols outlined by Ebuele, involving mixing ten grams of soil with 100 mL of Kelowna solution at pH 8.0 in a 250 mL Erlenmeyer flask [32].

Potentiometric measurements were conducted using standard phosphate-selective electrodes with concentrations ranging from 1.0×10^{-1} to 1.0×10^{-5} M and HPO_4^{2-} solutions prepared according to the ratios specified in Table 1. The pH effect on the electrode performance was investigated and the best response for HPO_4^{2-} species was obtained at pH 7.0 with good reproducibility. It differed slightly from the pH value (8.5) reported in the literature [33]. The slight change in the optimal pH for the electrode likely arose from a combination of factors related to differences in electrode composition, phosphate species distribution, surface chemistry, and experimental conditions. The modified electrode materials in our study may simply have had a different affinity for phosphate ions at a lower pH than the electrode used in previous studies. No variations were observed in the measurements obtained, especially with Composition 2 of these electrodes. Figure 4 illustrates the relationship between potential and concentration for the composite phosphate-selective electrode prepared with Composition 2. This specific composition was selected for performance evaluation due to its optimal potentiometric response and selectivity towards phosphate ions. The favorable performance of Composition 2 is attributed to its balanced epoxy content, which offers both mechanical stability and consistent ion exchange properties, ensuring reliable signal transduction.

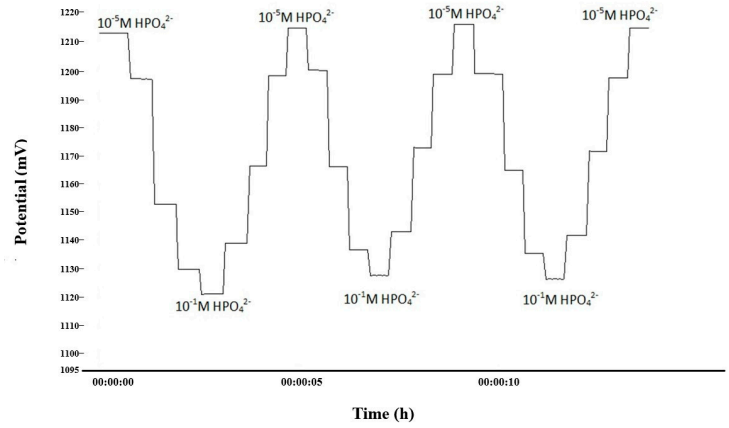

Figure 4. Potentiometric behavior of composite phosphate-selective electrode prepared with Ag-pGAP of composition.

The preparations of Compositions 1 and 3–5 were designed to systematically investigate how varying epoxy content influences potentiometric performance. The effects on membrane adhesion, electrical conductivity, and ion selectivity were examined by adjusting the epoxy ratios while keeping the amounts of CNT, Ag-pGAP, Ag_2S, and Cu_2S constant. Although not all compositions were evaluated in detail, preliminary testing showed that Composition 2 provided the best balance between selectivity, sensitivity, and stability. These findings led to the conclusion that Composition 2 was the most promising candidate for in-depth potentiometric analysis, resulting in the Nernstian response and high selectivity observed in this study.

Figure 5b presents the potentiometric response of the composite membrane phosphate-selective electrode prepared using Composition 2 listed in Table 1 against standard HPO_4^{2-} ions and other ions in the concentration range of 1.0×10^{-1} to 1.0×10^{-5} M.

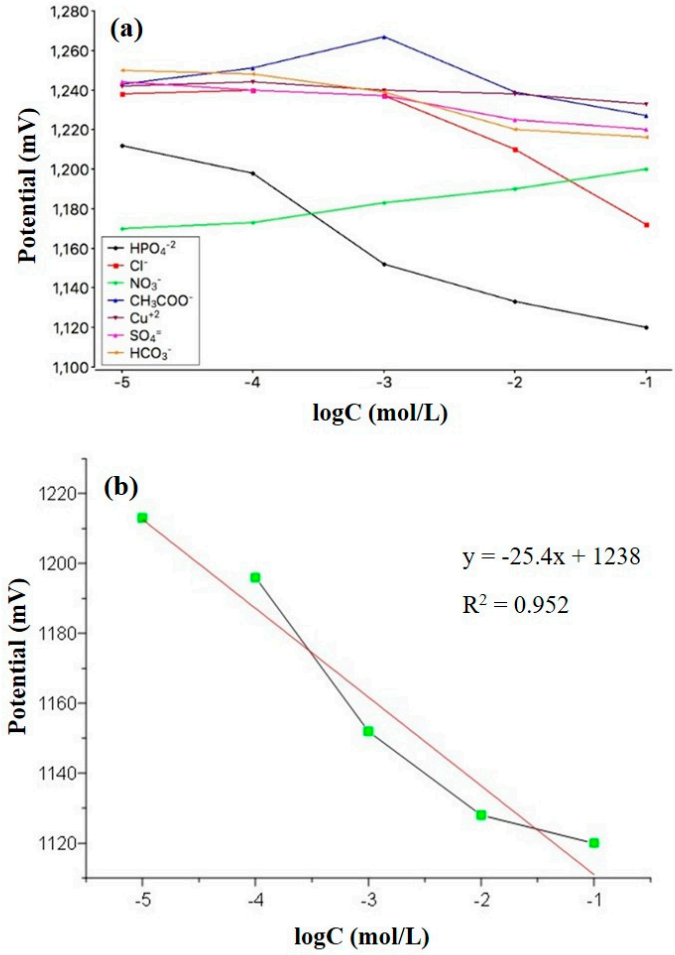

Figure 5. (**a**) Potentiometric behavior of the composite phosphate-selective electrode with Composition 2 towards ions HPO_4^{2-}, Cl^-, CH_3COO^-, Cu^{2+}, SO_4^{2-}, HCO_3^-, and NO_3^- (**b**) Calibration graph employed for determining the selectivity coefficient of the composite phosphate-selective electrode of Composition 2.

As shown in Figure 5a, the composite phosphate-selective electrode prepared using Composition 2 demonstrated specific sensitivity to HPO_4^{2-} ions, as well as to Cl^-, CH_3COO^-, Cu^{2+}, SO_4^{2-}, HCO_3^-, and NO_3^- ions. To better understand the selective behavior of the composite phosphate-selective electrode, selectivity coefficients were calculated. For this purpose, standard HPO4^{2-} solutions ranging from 1.0×10^{-1} to 1.0×10^{-5} M were prepared. The potential changes exhibited by the composite phosphate-selective electrode in response to these HPO_4^{2-} solutions were analyzed, and calibration curves were plotted using the obtained data. From the calibration curve, a linear equation was derived. Subsequently, the same electrode was employed to measure the potential changes in different standard anion solutions, including sodium and potassium, at concentrations ranging from 1.0×10^{-1} to 1.0×10^{-5} M. Selectivity coefficients were calculated based on the potential changes in each anion and the linear equation derived from the calibration curve. The calibration curve used for calculating selectivity coefficients is illustrated in Figure 5b.

Potentiometric measurements were conducted using a composite phosphate-selective electrode (Composition 2), which was prepared with silver polyglutaraldehyde phosphate. The electrode demonstrated a linear response to standard HPO_4^{2-} ions within a concentration range of 1.0×10^{-4} to 1.0×10^{-2} M at a pH of 7.0. The linear equation representing the potential–concentration relationship in the linear working range was determined as the following: $E = -25.4[HPO_4^{2-}] + 1238$ $R^2 = 0.952$. It was observed that within the linear

working range, there was an approximate 30 ± 1 mV potential difference for every 10-fold concentration change. The detection limit of the electrode with Composition 2 was determined to be 4.7 × 10^{-5} M. The results collectively demonstrate that the phosphate-selective composite electrode with Composition 2 not only provided a linear response but also showcased excellent sensitivity and a low detection limit for phosphate ions. In terms of repeatability, the electrode's performance was evaluated using standard HPO_4^{2-} solutions at concentrations of 1.0 × 10^{-2}, 1.0 × 10^{-3}, and 1.0 × 10^{-4} M. The measurements were conducted in a controlled environment, ensuring that the electrode surface was thoroughly washed with deionized water between different solutions to prevent cross-contamination. The potentiometric response behavior of the electrode is graphically presented in Figure 6 and numerically in Table 2, along with the standard deviations, to demonstrate the repeatability of the results.

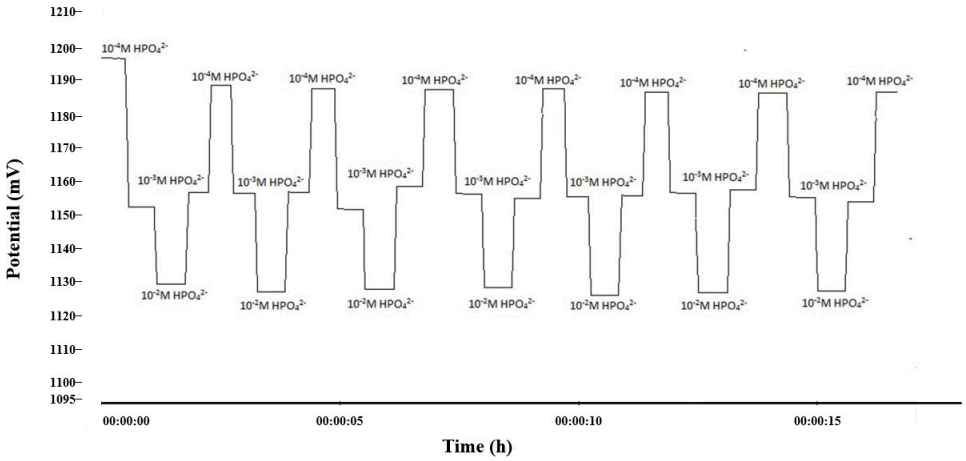

Figure 6. Reproducibility assessment of the composite phosphate-selective electrode with Composition 2, fabricated using Ag-pGAP.

Table 2. Average and standard deviation values showing the repeatability of the composite phosphate-selective electrode of Composition 2.

	Measurement Results (mV)							
HPO_4^{2-}	1	2	3	4	5	6	7	X ± S *
1 × 10^{-2} M	1130	1128	1128	1129	1127	1128	1128	1128.28 ± 0.95
1 × 10^{-3} M	1158	1158	1158	1153	1158	1157	1157	1157 ± 1.82
1 × 10^{-4} M	1189	1188	1188	1188	1187	1188	1188	1188 ± 0.58

* Average and standard deviation values are given for n = 7.

To measure the response time of the composite phosphate-selective electrode prepared with Ag-pGAP for Composition 2, the transition times to reach the equilibrium potential were examined in standard HPO_4^{2-} solutions within the concentration range of 1.0 × 10^{-1} to 1.0 × 10^{-5} M. The response time graph of the composite phosphate-selective electrode is shown in Figure 7. It was observed that the response time of the electrode, which exhibited repeatable and linear responses to standard HPO_4^{2-} ions in the concentration range of 1.0 × 10^{-2} to 1.0 × 10^{-4} M, was particularly less than 15 s, especially as the concentration increased towards higher concentrations.

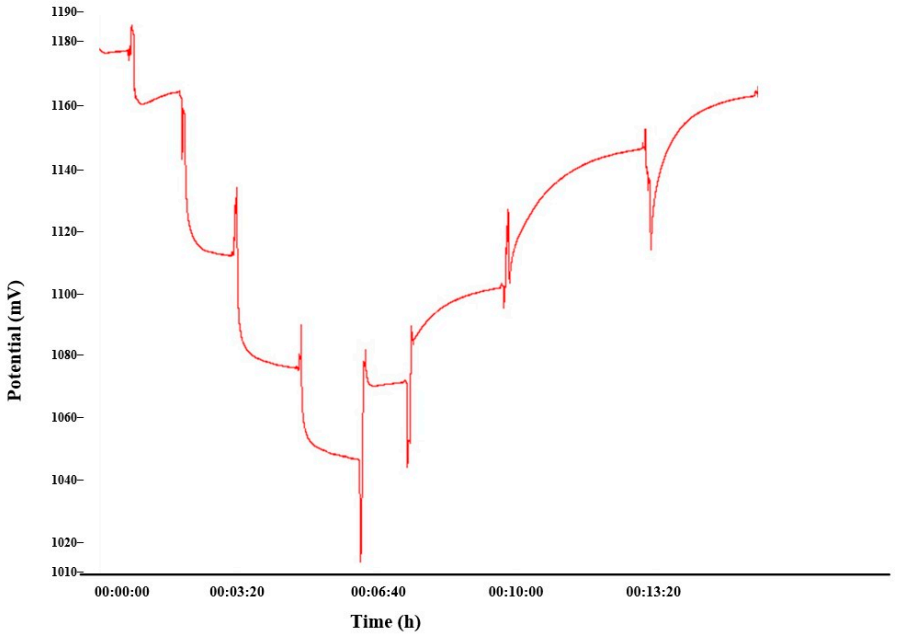

Figure 7. Response time of the composite phosphate-selective electrode prepared with Ag-pGAP, utilizing Composition 2.

3.6. Applications

The application section of this study involved the utilization of spectrophotometric [34] and potentiometric methods to extract separate PO_4^{3-} values from 30 soil samples collected from diverse locations in Istanbul. Extraction was carried out using Kelowna solution in Tris buffer at pH 8.0. Following extraction, the samples underwent filtration and were stored at room temperature for subsequent analysis using a solid-state phosphate-selective electrode. The acquired values underwent statistical assessment by employing the Bland–Altman method and regression technique [35]. Table 3 details descriptive statistics for the data obtained from the 30 soils, encompassing the mean, standard deviation, minimum, and maximum values for both the spectrophotometric (P_2O_5) and potentiometric (HPO_4^{2-}) methods.

Table 3. The descriptive statistics for the phosphate values obtained from the soil.

		n	Mean (ppm)	S.D.	Min.	Max.
Spectrophotometric	**P_2O_5**	30	2.35557	2.08279	0.28047	9.54652
Potentiometric	**HPO_4^{2-}**	30	2.29233	1.98941	0.3	9

In Table 3, the mean and standard deviation values of the data obtained through both measurement methods are very close to each other. The relevant data sets were initially subjected to the Bland–Altman method using the Origin program, and graphs depicting the deviations of the observed values from the mean were obtained, as shown in Figure 8.

Upon reviewing Figure 8, it is evident that the differences in the measurement results obtained by the two techniques do not exhibit a systematic distribution around the mean, but instead display a random distribution. According to the Bland–Altman method, the mean of the differences should be dispersed around zero. Therefore, using the Bland–Altman method, it was appropriate to assess the agreement between these two methods. The analysis indicated that there was an agreement between the two methods, and they could be considered as alternatives to each other. The results of the regression analysis of the relevant data sets are depicted in Figure 9. For the values, the fact that 99.7% of

the variation in either of the two methods could be explained by the other method (R^2) served as an indicator of the agreement, and the linearity ratio was also utilized to express the agreement.

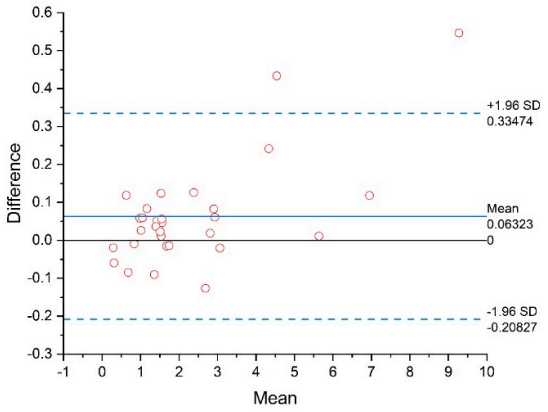

Figure 8. Bland–Altman plot obtained for the phosphate values for the comparison of measurement techniques.

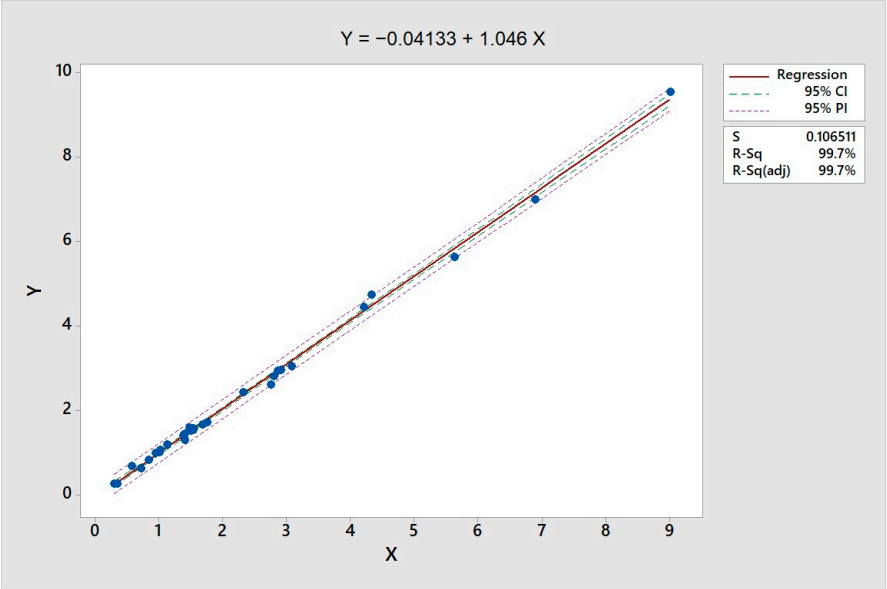

Figure 9. Regression plot obtained for the phosphate values for the comparison of measurement techniques. CI and PI represent 95% confidence intervals and prediction intervals, respectively.

The practical application of the composite phosphate-selective electrode was evaluated by examining soil surface water samples collected from three distinct agricultural regions near Istanbul. Initially, the water samples underwent filtration through 0.45 µm membranes, followed by analysis utilizing the standard addition method (Table 4).

Table 4. Determination of phosphate in soil surface water samples by the composite phosphate-selective electrode.

Sample	Phosphate Conc. (ppm)		Average *n*:7	SD±	CV (%)
	Min.	Max.			
Soil water 1	0.39	0.44	0.41	0.025	3.4
Soil water 2	0.35	0.42	0.39	0.035	5.6
Soil water 3	0.40	0.48	0.44	0.040	6.8

The results obtained from the electrode were compared with those from the conventional spectrophotometric method for determining dissolved phosphate levels (Table 5).

Table 5. Comparison of the results obtained by the composite phosphate-selective electrode and UV-Vis spectrophotometry.

Sample	Phosphate Conc., ppm, *n*:3	
	The Electrode	UV-Vis
Soil water 1	0.42	0.45
Soil water 2	0.38	0.40
Soil water 3	0.45	0.42

To validate the correlation between the two methods, statistical tests such as Student's *t*-test and Fisher's F-test were employed, with calculated values provided [36]. Remarkably, the experimental *t*-test and F-test values for phosphate were found to be lower than the theoretical values (*t*-test = 4.0, $n = 7$; F-test = 17.0, $n = 7$), with a confidence level of 95% ($p < 0.05$). This suggests that the proposed composite phosphate-selective electrode yields results that agree with the preferred spectrophotometry method.

The results obtained from the filtered soil surface water samples showed a strong correlation with those obtained from the preferred spectrophotometry method, indicating the high suitability of the proposed composite phosphate-selective electrode for sensing phosphate levels in real agricultural wastewater. This finding highlights its potential for practical applications in monitoring and evaluating phosphate content in soil surface water sources.

Overall, this study presents the development of a novel composite phosphate-selective electrode that employs a matrix of Ag-pGAP and CNT for the on-site and real-time detection of phosphate in various environmental applications [37]. The composite material was synthesized through a chemical reaction involving thiourea dioxide, glutaraldehyde, and silver nitrate ($AgNO_3$), followed by precipitation with disodium monohydrogen phosphate (Na_2HPO_4). The resulting structure integrates silver polyglutaraldehyde phosphate, silver sulfide (Ag_2S), and copper sulfide (Cu_2S) with epoxy as a binding agent, thereby optimizing stability, sensitivity, and selectivity for phosphate detection.

Characterization techniques, including Fourier-transform infrared spectroscopy (FTIR), scanning electron microscopy (SEM), X-ray diffraction (XRD), and thermogravimetric analysis (TGA), confirmed the successful formation of the composite, demonstrating its structural integrity and thermal stability [38]. The electrode exhibited a linear potentiometric response to phosphate ion concentrations ranging from 1.0×10^{-4} M to 1.0×10^{-2} M, showing high selectivity against other anions such as chloride and nitrate, indicating its suitability for application in complex environmental matrices.

The electrode's rapid response time of less than 15 s is essential for real-time monitoring, and its performance was validated against traditional spectrophotometric methods, revealing a strong correlation in phosphate detection from surface water and soil samples [39]. This underscores the electrode's accuracy and its potential to complement or replace conventional laboratory techniques. Its application in agricultural regions near Istanbul highlights its role in mitigating phosphate-related environmental issues, such as eutrophication, while optimizing fertilizer usage.

Moreover, the electrode's portability, cost-effectiveness, minimal sample preparation requirements, and environmental friendliness enhance its practicality for in-field measurements [40]. Statistical analyses, including the Bland–Altman method, regression analysis, Student's *t*-test, and Fisher's F-test, confirmed the reliability of the results, ensuring that observed differences between methods were statistically insignificant [41].

4. Conclusions

The developed CNT/Ag-pGAP composite electrode demonstrated high sensitivity, selectivity, and stability for detecting phosphate ions. It exhibited a Nernstian response across a concentration range of 1.0×10^{-4} M to 1.0×10^{-2} M. This range effectively covers the typical phosphorus concentrations in soil water samples.

The selectivity of the electrode was validated against six common interfering ions: Cl^-, CH_3COO^-, Cu^{2+}, $SO_4{}^{2-}$, $HCO_3{}^-$, and $NO_3{}^-$. The results showed that the electrode responded significantly more to phosphate ions than these interfering ions.

Potentiometric measurements indicated good reproducibility, particularly for Composition 2, which balanced mechanical stability and consistent ion exchange properties, ensuring reliable signal transduction. The optimal performance was observed at pH 7.0, which slightly differs from previous studies; this variation was attributed to differences in electrode composition and surface chemistry.

In real-world applications, the electrode demonstrated robust performance in areas such as water quality management and agricultural monitoring, confirming its suitability for on-site and real-time environmental monitoring. Its potential for scaling and practical deployment positions this electrode as an effective and reliable solution for phosphate detection, thereby contributing to improved environmental management and agricultural productivity.

Author Contributions: O.T.: Conceptualization, data curation, investigation, methodology, visualization, writing—review, editing, and original draft. V.E.: Data curation, methodology, writing—review and editing. F.C.: Investigation, methodology, data curation, writing—review, editing, and original draft. I.I.: Project administration, supervision, writing—review and editing. M.Z.K.: Investigation, methodology, writing—review and editing. All authors have read and agreed to the published version of the manuscript.

Funding: This research received no external funding.

Institutional Review Board Statement: Not applicable.

Data Availability Statement: Data supporting the reported results are available upon reasonable request from the corresponding author.

Acknowledgments: This research was funded by the General Directorate of Agricultural Research and Policies (TA-GEM), grant number TAGEM-19/AR-GE/04.

Conflicts of Interest: The authors declare no conflicts of interest.

References

1. Chen, J.; Li, D.; Ding, X.; Zhang, D. Sensitive and selective electrochemical aptasensing method for the voltammetric determination of dopamine based on AuNPs/PEDOT-ERGO nanocomposites. *Bioelectrochemistry* **2024**, *157*, 108653. [CrossRef] [PubMed]
2. Palo, E.; Zhang, H.; Lastusaari, M.; Salomäki, M. Nanometer-Thick Ion-Selective Polyelectrolyte Multilayer Coatings to Inhibit the Disintegration of Inorganic Upconverting Nanoparticles. *ACS Appl. Nano Mater.* **2020**, *3*, 6892–6898. [CrossRef]
3. Saikrithika, S.; Kumar, S. A selective voltammetric pH sensor using graphitized mesoporous carbon/polyaniline hybrid system. *J. Chem. Sci.* **2021**, *133*, 2. [CrossRef]
4. Daneshgar, S.; Callegari, A.; Capodaglio, A.G.; Vaccari, D. The potential phosphorus crisis: Resource conservation and possible escape technologies: A review. *Resources* **2018**, *7*, 37. [CrossRef]
5. Kates, D.M.; Sherrard, D.J.; Andress, D.L. Evidence that serum phosphate is independently associated with serum PTH in patients with chronic renal failure. *Am. J. Kidney Dis.* **1997**, *30*, 809–813. [CrossRef] [PubMed]
6. Desmeules, S.; Bergeron, M.J. Isenring. Acute Phosphate Nephropathy and Renal Failure. *N. Engl. J. Med.* **2003**, *349*, 1006–1007. [CrossRef]
7. Kim, D.Y.; Kim, D.G.; Jeong, B.; Kim, Y.I.; Heo, J.; Lee, H.K. Reusable and pH-Stable Luminescent Sensors for Highly Selective Detection of Phosphate. *Polymers* **2022**, *14*, 190. [CrossRef]

8. Tang, C.; Fu, D.; Wang, R.; Zhang, X.; Wei, L.; Li, M.; Li, C.; Cao, Q.; Chen, X. An Electrochemical Microfluidic System for on-Site Continuous Monitoring of Soil Phosphate. *IEEE Sens. J.* **2024**, *24*, 6754–6764. [CrossRef]
9. Parra, A.; Ramon, M.; Alonso, J.; Lemos, S.G.; Vieira, E.C.; Nogueira, A.R.A. Flow injection potentiometric system for the simultaneous determination of inositol phosphates and phosphate: Phosphorus nutritional evaluation on seeds and grains. *J. Agric. Food Chem.* **2005**, *53*, 7644–7648. [CrossRef]
10. Ganjali, M.R.; Norouzi, P.; Ghomi, M.; Salavati-Niasari, M. Highly selective and sensitive monohydrogen phosphate membrane sensor based on molybdenum acetylacetonate. *Anal. Chim. Acta* **2006**, *567*, 196–201. [CrossRef]
11. Akyilmaz, E.; Yorganci, E. Construction of an amperometric pyruvate oxidase enzyme electrode for determination of pyruvate and phosphate. *Electrochim. Acta* **2007**, *52*, 7972–7977. [CrossRef]
12. Kwan, R.C.H.; Leung, H.F.; Hon, P.Y.T.; Barford, J.P.; Renneberg, R. A screen-printed biosensor using pyruvate oxidase for rapid determination of phosphate in synthetic wastewater. *Appl. Microbiol. Biotechnol.* **2005**, *66*, 377–383. [CrossRef] [PubMed]
13. Zhao, H.X.; Liu, L.Q.; de Liu, Z.; Wang, Y.; Zhao, X.J.; Huang, C.Z. Highly selective detection of phosphate in very complicated matrixes with an off–on fluorescent probe of europium-adjusted carbon dots. *Chem. Commun.* **2011**, *47*, 2604–2606. [CrossRef] [PubMed]
14. Preechaworapun, A.; Dai, Z.; Xiang, Y.; Chailapakul, O.; Wang, J. Investigation of the enzyme hydrolysis products of the substrates of alkaline phosphatase in electrochemical immunosensing. *Talanta* **2008**, *76*, 424–431. [CrossRef]
15. Mousty, C.; Cosnier, S.; Shan, D.; Mu, S. Trienzymatic biosensor for the determination of inorganic phosphate. *Anal. Chim. Acta* **2001**, *443*, 1–8. [CrossRef]
16. Mahmud, M.A.P.; Ejeian, F.; Azadi, S.; Myers, M.; Pejcic, B.; Abbassi, R.; Razmjou, A.; Asadnia, M. Recent progress in sensing nitrate, nitrite, phosphate, and ammonium in aquatic environment. *Chemosphere* **2020**, 259. [CrossRef]
17. Berchmans, S.; Issa, T.B.; Singh, P. Determination of inorganic phosphate by electroanalytical methods: A review. *Anal. Chim. Acta* **2012**, *729*, 7–20. [CrossRef]
18. Ebadi, M.; Asareh, A.; Yengejeh, R.J.; Hedayat, N. Investigation of electro-coagulation process for phosphate and nitrate removal from sugarcane wastewaters. *Iran. J. Toxicol.* **2021**, *15*, 19–26. [CrossRef]
19. Lawrence, N.S.; Beckett, E.L.; Davis, J.; Compton, R.G. Advances in the voltammetric analysis of small biologically relevant compounds. *Anal. Biochem.* **2002**, *303*, 1–16. [CrossRef]
20. Hart, J.P.; Crew, A.; Crouch, E.; Honeychurch, K.C.; Pemberton, R.M. Some Recent Designs and Developments of Screen-Printed Carbon Electrochemical Sensors/Biosensors for Biomedical, Environmental, and Industrial Analyses. *Anal. Lett.* **2004**, *37*, 789–830. [CrossRef]
21. Pan, D.; Wang, Y.; Chen, Z.; Lou, T.; Qin, W. Nanomaterial/ionophore-based electrode for anodic stripping voltammetric determination of lead: An electrochemical sensing platform toward heavy metals. *Anal. Chem.* **2009**, *81*, 5088–5094. [CrossRef] [PubMed]
22. Manjunatha, J.G.; Deraman, M.; Basri, N.H.; Talib, I.A. Fabrication of poly (Solid Red A) modified carbon nano tube paste electrode and its application for simultaneous determination of epinephrine, uric acid and ascorbic acid. *Arab. J. Chem.* **2018**, *11*, 149–158. [CrossRef]
23. Wardak, C.; Pietrzak, K.; Morawska, K.; Grabarczyk, M. Ion-Selective Electrodes with Solid Contact Based on Composite Materials: A Review. *Sensors* **2023**, *23*, 5839. [CrossRef] [PubMed]
24. Khairuddin, R.; Andarini, N.; Oktriviani, W.; Toda'A, M.; Kaope, V.H. Study of Phosphate Adsorption Using Ferrihydrite with Diffusive Gradient in Thin Films Method. *IOP Conf. Ser. Earth Environ. Sci.* **2022**, *1075*, 1. [CrossRef]
25. Vardar, G.; Altikato̧lu, M.; Ortaç, D.; Cemek, M.; Işildak, I. Measuring calcium, potassium, and nitrate in plant nutrient solutions using ion-selective electrodes in hydroponic greenhouse of some vegetables. *Biotechnol. Appl. Biochem.* **2015**, *62*, 663–668. [CrossRef]
26. Dai, J.; Zhu, Y.; Tahini, H.A.; Lin, Q.; Chen, Y.; Guan, D.; Zhou, C.; Hu, Z.; Lin, H.-J.; Chan, T.-S.; et al. Single-phase perovskite oxide with super-exchange induced atomic-scale synergistic active centers enables ultrafast hydrogen evolution. *Nat. Commun.* **2020**, *11*, 1. [CrossRef]
27. Savale, P.A. Comparative Study of POA-PVS-DBS-GOD Electrode in Acetate and Phosphate Buffers for Determination of Glucose. *Adv. Sci. Lett.* **2018**, *24*, 5759–5763. [CrossRef]
28. Hamidah, L.N.; Afkar, K.; Rahmayanti, A.; Fitrianah, L. Performance of slow sand filter reactor using geotextile for reducing total n and phosphate. *in IOP Conf. Ser. Earth Environ. Sci.* **2022**, *1211*, 1. [CrossRef]
29. Guan, D.; Xu, H.; Huang, Y.; Jing, C.; Tsujimoto, Y.; Xu, X.; Lin, Z.; Tang, J.; Wang, Z.; Sun, X.; et al. Operando Studies Redirect Spatiotemporal Restructuration of Model Coordinated Oxides in Electrochemical Oxidation. *Adv. Mater.* **2024**, 2413073. [CrossRef]
30. Staaks, D.; Olynick, D.L.; Rangelow, I.W.; Altoe, M.V.P. Polymer-metal coating for high contrast SEM cross sections at the deep nanoscale. *Nanoscale* **2018**, *10*, 22884–22895. [CrossRef]

31. Kozlovskaya, V.; Zavgorodnya, O.; Chen, Y.; Ellis, K.; Tse, H.M.; Cui, W.; Thompson, J.A.; Kharlampieva, E. Ultrathin polymeric coatings based on hydrogen-bonded polyphenol for protection of pancreatic islet cells. *Adv. Funct. Mater.* **2012**, *22*, 3389–3398. [CrossRef]
32. Prakasham, R.S.; Kumar, B.S.; Kumar, Y.S.; Shankar, G.G. Characterization of silver nanoparticles synthesized by using marine isolate Streptomyces albidoflavus. *J. Microbiol. Biotechnol.* **2012**, *22*, 614–621. [CrossRef] [PubMed]
33. Ebuele, V.O.; Congrave, D.G.; Gwenin, C.D. Fitzsimmons-Thoss. Development of a Cobalt Electrode for the Determination of Phosphate in Soil Extracts and Comparison with Standard Methods. *Anal. Lett.* **2018**, *51*, 834–848. [CrossRef]
34. Forano, C.; Farhat, H. Mousty. Recent trends in electrochemical detection of phosphate in actual waters. *Curr. Opin. Electrochem.* **2018**, *11*, 55–61. [CrossRef]
35. Hall, L.B. A text-book of quantitative chemical analysis. *J. Am. Chem. Soc.* **1903**, *25*, 318–319. [CrossRef]
36. Ziegel, E.R. Statistics and Chemometrics for Analytical Chemistry. *Technometrics* **2004**, *46*, 498–499. [CrossRef]
37. Meruva, R.K.; Meyerhoff, M.E. Mixed potential response mechanism of cobalt electrodes toward inorganic phosphate. *Anal. Chem.* **1996**, *68*, 2022–2026. [CrossRef]
38. Topcu, C.; Caglar, B.; Onder, A.; Coldur, F.; Caglar, S.; Guner, E.K.; Cubuk, O.; Tabak, A. Structural characterization of chitosan-smectite nanocomposite and its application in the development of a novel potentiometric monohydrogen phosphate-selective sensor. *Mater. Res. Bull.* **2018**, *98*, 288–299. [CrossRef]
39. Özkütük, E.B.; Yıldız, B.; Gündüz, M.; Hür, E. Phosphate-imprinted polymer as an efficient modifier for the design of ion-selective electrode. *J. Chem. Technol. Biotechnol.* **2021**, *96*, 2604–2609. [CrossRef]
40. Bhat, K.S.; Nakate, U.T.; Yoo, J.Y.; Wang, Y.; Mahmoudi, T.; Hahn, Y.B. Nozzle-Jet-Printed Silver/Graphene Composite-Based Field-Effect Transistor Sensor for Phosphate Ion Detection. *ACS Omega* **2019**, *4*, 8373–8380. [CrossRef]
41. Ratkovski, G.P.; Nascimento, K.T.O.D.; Pedro, G.C.; Ratkovski, D.R.; Gorza, F.D.S.; da Silva, R.J.; Maciel, B.G.; Mojica-Sánchez, L.C.; de Melo, C.P. Spinel Cobalt Ferrite Nanoparticles for Sensing Phosphate Ions in Aqueous Media and Biological Samples. *Langmuir* **2020**, *36*, 2920–2929. [CrossRef] [PubMed]